ELSEVIER

Global and Planetary Change 35 (2002) 67–74

GLOBAL AND PLANETARY CHANGE

www.elsevier.com/locate/gloplacha

Patterns and frequencies of the East Asian winter monsoon variations during the past million years revealed by wavelet and spectral analyses

Huayu Lu[a,*], Fuqing Zhang[b], Xiaodong Liu[a]

[a]*State Key Laboratory of Loess and Quaternary Geology, Institute of Earth Environment, Chinese Academy of Sciences, No. 10, Fenghui Nanlu, Xi'an high-tech zone, Xi'an 710075, China*

[b]*Department of Atmospheric Sciences, Texas A&M University, College Station, TX, 77843-3150, USA*

Received 1 February 2000; received in revised form 21 August 2001; accepted 20 March 2002

Abstract

The wavelet and spectral analyses are used to investigate the variations of patterns and frequencies of the East Asian winter monsoon system during the past million years. Grain size of the loess–paleosol deposit at the central Chinese Loess Plateau is employed as a proxy indicator of the winter monsoon strength. On the bases of palaeomagnetic dates and a sedimentation rate model, an absolute, not orbitally tuned time scale for the loess deposit is developed. Wavelet analyses on this time series show that the patterns and frequencies of the East Asian winter monsoon climate vary with time during the past million years. The wavelet analyses also revealed a shift of climatic pattern from predominantly quasi-200- to quasi-100-ka cycle at around 500 ka BP which is also supported by previous studies using the sedimentation rate analysis as well as paleosol observations. Traditional spectral analysis on the same time series shows that the East Asian winter monsoon changes at Milankovich cycles, but there are also cycles which may not be related to orbital forcing. The predominant 41-ka cycle identified from previous studies is not evident in this time series from both wavelet and spectral analyses. Our results present new evidence that not only solar radiation, but also other boundary conditions, may have forced the monsoon system changes at the 10^4–10^5 years time scale.

Keywords: East Asian palaeomonsoon; Pleistocene epoch; wavelet analysis; Chinese loess

1. Introduction

East Asian monsoon variations revealed by Chinese loess deposit have been investigated by many researchers. Analyses of frequency and pattern of the monsoon system changes at 10^4–10^5-year time scale have showed that the winter monsoon variations were mostly forced by the solar radiation and the ice volume changes in the northern hemisphere during the Pleistocene (Li et al., 1988; An et al., 1990; Xu and Liu, 1994; Ding et al., 1994, 1995; Porter and An, 1995; Morley and Heusser, 1997; Van Huissteden et al., 1997; Liu and Ding, 1998; Lu et al., 1999a). However, controversies with respect to the patterns and frequencies of the monsoon changes on orbital time scales still exist. These may be caused by (1) use of parameters of which the climatic implication is unclear; (2) use of inaccurate time scales; (3) use of

* Corresponding author. Tel.: +86-29-832-1862; fax: +86-29-832-0456.

E-mail address: luhy@loess.llqg.ac.cn (H. Lu).

0921-8181/02/$ - see front matter
PII: S0921-8181(02)00136-4

different mathematical tools; and (4) a combination of these aspects. For example, the spectral analysis results on magnetic susceptibility time series by Kukla et al. (1990), Wang et al. (1990), An et al. (1990) and Xu and Liu (1994) have been challenged by Zhou et al. (1990) and Maher and Thompson (1992) because of the physical mechanisms in their age models and the climatic implications of the proxy index (magnetic susceptibility) used are unclear. Recently, Van Huissteden et al. (1997) used a grain-size time series and a sedimentation rate model with compaction correction to establish an absolute chronology for the loess deposit, and the time series was analyzed by maximum entropy spectrum analysis (MESA) and Thompson's multitaper method (MTM). The results show significant orbital cycles in the monsoon system. They also identified other cycles from the time series that cannot be explained by the orbital forcing. However, their mathematical tools cannot examine the cycle variation over time. Here, we reexamine the patterns and frequencies of the East Asian winter monsoon climate recorded by the loess–palesol deposit at the central Chinese Loess Plateau. The grain size is used as the proxy indicator that has clear climatic implication. An absolute, not orbitally tuned time series for the loess deposit is developed as well. Both the continuous wavelet transform (CWT) and the classical spectral analysis (Blackman–Tukey method) are used to reveal the variations of patterns and frequencies of the East Asian winter monsoon system during the past million years.

2. Data and methodology

A 70-m-thick loess–paleosol exposure at Luochuan, central Chinese Loess Plateau is sampled at 5- or 10-cm intervals with an average time resolution of 0.7–1.4 ka. All the samples are measured for grain-size distribution (Vandenberghe et al., 1997; Van Huissteden et al., 1997; Lu et al., 1999b) (Fig. 1a). Modern dust storm and dust fall events in northern China are associated with strong northwest winds, occur mainly in spring and winter and historically are associated with dry and cold intervals (Liu, 1985; An et al., 1991; Porter and An, 1995). When the winter monsoon circulation is strengthened, the wind circulation brings coarse particle dust from the arid/semi-arid desert and the Gobi region in inland China southeastward to the Loess Plateau. Therefore, the grain size of the loess deposit is strongly related to the winter monsoon strength. Geological investigation and modern climatic analyses indicated that during a cold-phase climate such as a glacial period, dust storm events are more frequent, and the grain size of the dust is coarser due to the strengthened winter monsoon (Zhang et al., 1994, 1999; Lu et al., 1997; Liu and Ding, 1998). The grain size of the loess–paleosol deposit is, therefore, regarded as a good proxy index of the winter monsoon strength. In order to find a sensitive proxy index of the winter monsoon strength, the grain-size distribution of each sample of the last glacial cycle is divided into 42 fractions of 0.25 phi wide. The grain-size variations then were compared to the geological record (Liu, 1985). The results show that the coarse fraction with grain size greater than 30 μm is a sensitive indicator of the winter monsoon changes (Lu et al., 1997, 1999b). This may be explained by the observations that the coarse fraction particles are mostly aeolian origin, but the finer fraction such as the clay fraction may be partly formed by the post depositional weathering and pedogenesis process (Sun et al., 2000). Therefore, the >30 μm particles are less modified, and thus employed as the proxy index of the winter monsoon strength in this study.

Thermoluminescence (TL) dates and palaeomagnetic reversal ages offer absolute dates to the loess–palaeosol sequence (Kukla and An, 1989; Forman, 1991). The results are then used as age control points in order to develop an absolute and detailed time series. The sedimentation rate model developed by Porter and An (1995) is employed to calculate the age of each sampling point. Since the dust sedimentation rate is positively proportional to the particle size (An et al., 1991; Zhang et al., 1994, 1999; Porter and An, 1995), the grain size of stratigraphic intervals is reversely proportional to its duration. Thus, the age of each sampling level can be obtained by the following model (Porter and An, 1995):

$$T_m = T_1 + (T_2 - T_1)\left(\sum_{i=1}^{m} A_i^{-1} \Big/ \sum_{i=1}^{n} A_i^{-1}\right)$$

where T_1 and T_2 are the ages of the control points, A_i is the accumulation rate at any level i which is

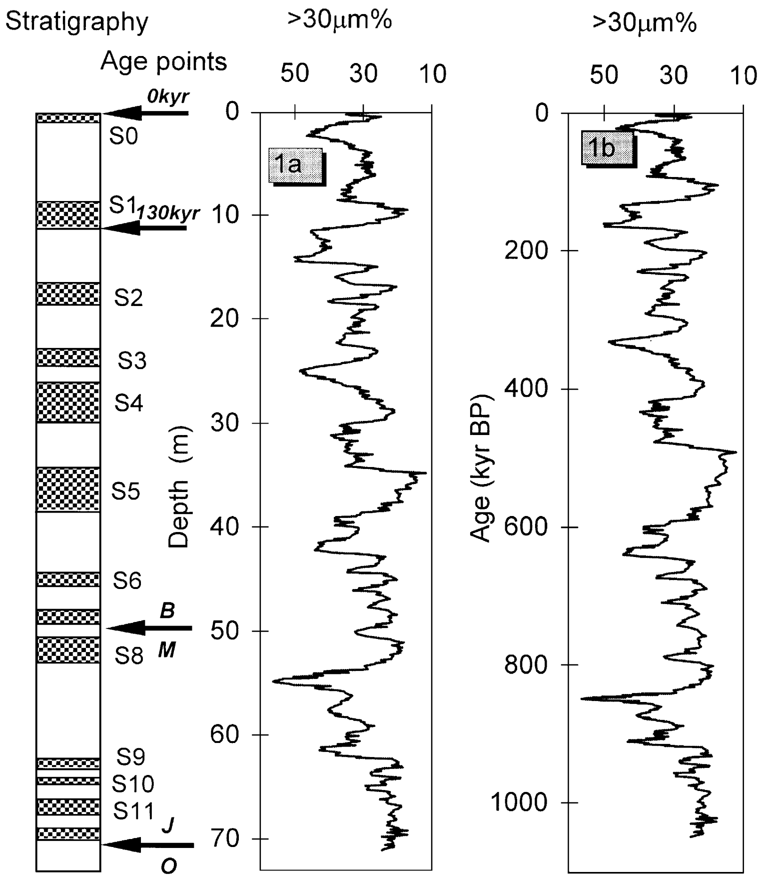

Fig. 1. Stratigraphy of the loess–paleosol deposit at Luochuan, Chinese Loess Plateau. Age control points and the >30-μm coarse fraction (%) changes plotted (a) against depth and (b) against the absolutely detailed (not orbitally tuned) time scale.

assumed to be proportional to the >30-μm fraction, n is the sampling level between T_1 and T_2 and m is the sampling level in T_1 and T_2. One modification here is that the >30-μm size fraction is assumed to be proportional to the accumulation rate rather than the >40-μm size fraction because the detailed analysis of the grain-size distribution of the loess deposit at Luochuan shows the >30 μm is more strongly associated with the winter monsoon strength (Lu et al., 1997, 1999b) and thus the dust flux and the sedimentation rate (Lu et al., 2000). Four absolute age controls are used in the calculation. The age of the top of the stratigraphy is 0 ka BP. The age of bottom of the first paleosol unit (S1) is 130 ka BP (Kukla and An, 1989; An et al., 1991; Forman, 1991). The Brunhess/Matuyama (B/M) and Jaramillo/Matuyama (J/M) boundaries are located at the 8th loess unit (L8) and the 13th loess unit (L13) and are dated at 780 and 1049 ka BP, respectively (Kukla and An, 1989; Cande and Kent, 1992). By this way, a new grain-size time series, which should be a good proxy index of the winter monsoon strength variation in the past million years, is obtained (Fig. 1b).

The wavelet transform is a relatively new data analysis tool and has been shown to be very useful in analysis of geophysical time series (Weng and Lau, 1994; Bolton et al., 1995; Lau and Weng, 1995; Liu and Chao, 1998). One of the advantages of the wavelet transform over the traditional spectrum analysis tools of Fourier transform and maximum entropy analysis is that it can provide flexible localized time-frequency (or space-wavelength) information. Basically, the wavelet transform uses a set of functions (wavelet functions) to express a signal of time series. Wavelet functions can be obtained by smoothly moving, expanding or contracting a function, and the coefficients of the wavelet function by the transform can depict the original function (Weng and Lau, 1994). The wavelet transform can examine changes of the frequency and pattern of time series with time. However, the traditional spectral analysis tools can only examine the frequency as a whole time series. Therefore, the wavelet transform could offer new information of the cycle evolution of time series.

Discrete wavelet transform and continuous wavelet transform are two fundamental kinds of wavelet analysis. Continuous wavelet transform is more suitable for most real-valued geophysical time series (Weng and Lau, 1994). By using the continuous wavelet transform, we can project the original signal to any frequency (or cycle) domain and thereby obtain the amplitude and phase in frequency space. The continuous wavelet transform of a square integrable function *f* is defined as

$$W_f(a,b) = \langle f, I^*_{a,b} \rangle = a^{-1/2} \int_{-\infty}^{+\infty} f(t) I^* \left(\frac{t-b}{a} \right) \mathrm{d}t$$

where I is the base wavelet function, the asterisk denotes a complex conjugate, a is the dilation parameter and b is the translation parameter (Weng and Lau, 1994).

Continuous wavelet transform was used for this study. The most widely used Morlet function

$$I(t) = \mathrm{e}^{ik_I t} \mathrm{e}^{-\left(|t|^2/2\right)}$$

was chosen to be the basic wavelet function, which is a plane wave of wave vector I modulated by a Gaussian envelope of unit width. A practical algorithm for continuous wavelet transform using Morlet function as the base wavelet can be found in Weng and Lau (1994). The wavelet transform was performed with the continuous wavelet transform package accompanying MATLAB@.

Classical spectral analyses are also performed on the winter monsoon time series in order to compare with CWT. The Blackman and Tukey (1958) method gives an estimate of the power spectrum of a given time series. More specifically, the power spectrum is equal to the Fourier transform of the autocorrelation. The Blackman–Tukey method can help in reducing the spectral estimate's variance and bias, and attenuate the leakage effects of the periodogram. This is a simple and efficient method of spectral estimate, especially for estimating the continuous part of the spectrum. However, this tool is less useful for the detection of components of the signal that is purely sinusoidal or nearly so because of its low resolution and frequency dependence of errors (Ghil et al., submitted for publication). We analyze time series covering 1024–0, 1000–500 and 500–0 ka to see the frequency evolutions and disadvantages of the traditional spectral method.

3. Variations of the winter monsoon at multitime scales

A continuous spectrum at any time can be achieved using continuous wavelet transform (CWT, Weng and Lau, 1994). We have decomposed the absolute time series (Fig. 1b) by CWT with an emphasis on the detection of periodic variation ranging from 10 to 250 ka. The continuous wavelet coefficients are shown in Fig. 2 indicating the frequencies and patterns of the winter monsoon variations during the past 1024 ka with time. Positive (negative) values correspond to the strong (weak) winter monsoon anomaly.

From Fig. 2, we can see that there is a relatively consistent and strong 130–100 (quasi-100)-ka cycle over the entire time series. There is also a predominant quasi-200-ka cycle during the 1024–500 ka BP period, but this quasi-200-ka cycle is gradually overtaken by the quasi-100-ka cycle during the last 500 ka. The winter monsoon system changes to a higher amplitude variation during the 500–0 ka BP with distinct contrast to that between 1024 and 500 ka BP. Fig. 2 also indicates a relatively weak and varying 60–50-ka cycle during 950–750 and 350–0 ka BP. There is a consistent 25–18-ka cycle over the entire time series, but not equally strong over the entire time series. It appears to be stronger during 850–950, 600–700 and around 200 ka (Fig. 2). However, the 41-ka cycle, which is considered as one of the most important cycles of the orbital forcing in the northern hemispheric climate, is not evident from the CWT of this not orbitally tuned time series. Possible reasons for this non-41-ka-cycle time series will be discussed in Section 4.

We also conducted a classical spectral analysis on this time series (Blackman and Tukey, 1958) to

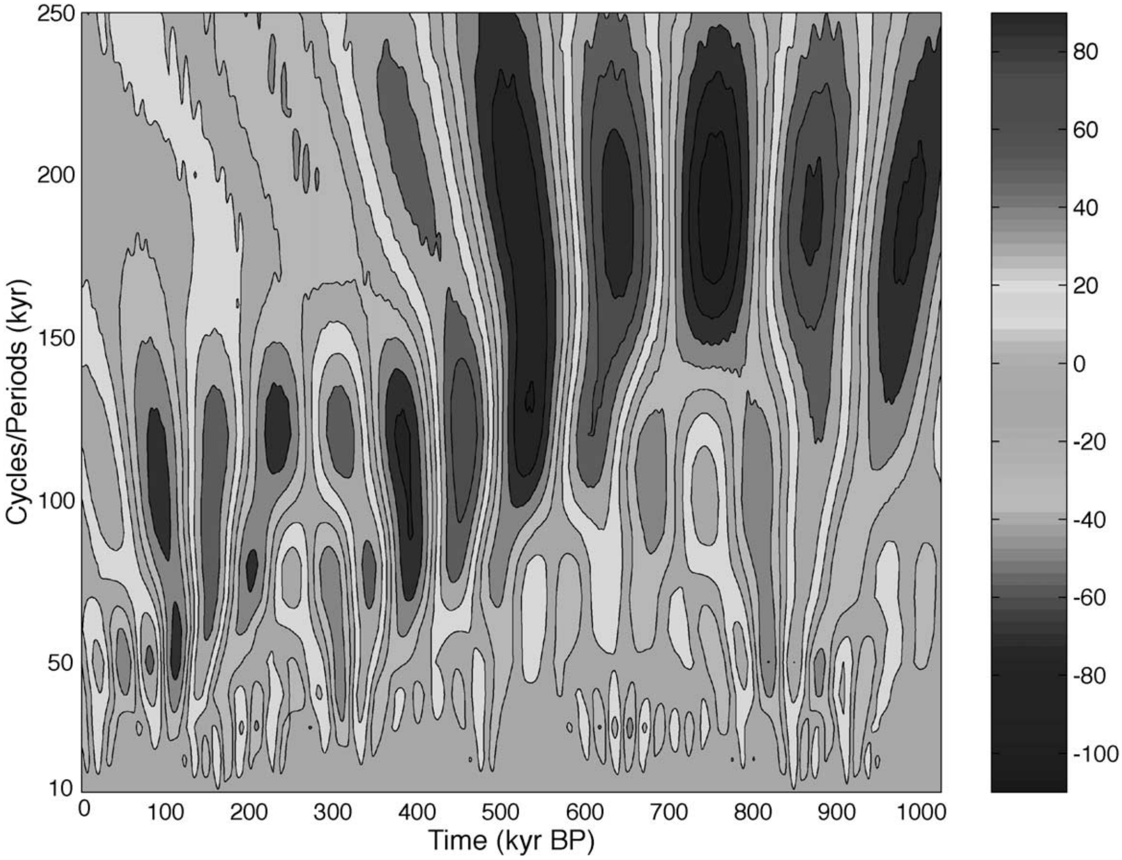

Fig. 2. Wavelet coefficients of the continuous wavelet transform of the time series shown in Fig. 1b. The contour interval is 20 from − 110 to 90 with no zero lines; positive (negative) value indicates stronger (weaker) winter monsoon variation contributed relatively from any given cycle/period (*Y*-axis) at any given time (*X*-axis).

compare with the wavelet analyses. The spectral analyses covering 1024–0 ka show that there are quasi-100-, quasi-55-, 35- and 23-ka cycles that are significantly above the 95% confidence level; during the 500–0 ka, the quasi-100- and 55-ka cycles are very strong, but these cycles are not significant during 1000–500 ka (Fig. 3). The previously found 41-ka cycle is not presented by our spectral analysis. In general, both methods agree with each other though the spectral method lacks the detail of the frequency variation over time. The quasi-100-, 55-, 35- and 23-ka cycles found from the spectral analyses are evident in the wavelet analyses with varying strength and time. The quasi-100- and 23-ka cycles may be related to the Milankovich cycles, the cause of 55-ka (close to the orbital 56 ka) cycles and 35-ka cycle may be orbitally or nonorbitally forced.

Previous investigators have also reported the non-orbital frequencies of the East and South Asian monsoons changes in Pleistocene with different explanations (Pisias and Rea, 1988; An et al., 1990; Wang et al., 1990; Kukla et al., 1990; Clemens et al., 1991; Xu and Liu, 1994; Van Huissteden et al., 1997). One explanation is that these frequencies are derived from inaccurate time scales; the other explanation is that these frequencies may originate from interaction of the monsoon component with an internal forcing of the climate system. Although the detailed mechanism is still unclear, the presence of frequencies of non-orbital forcing is suggested. Also, harmonics or combination tones modifying extra-forcing frequencies

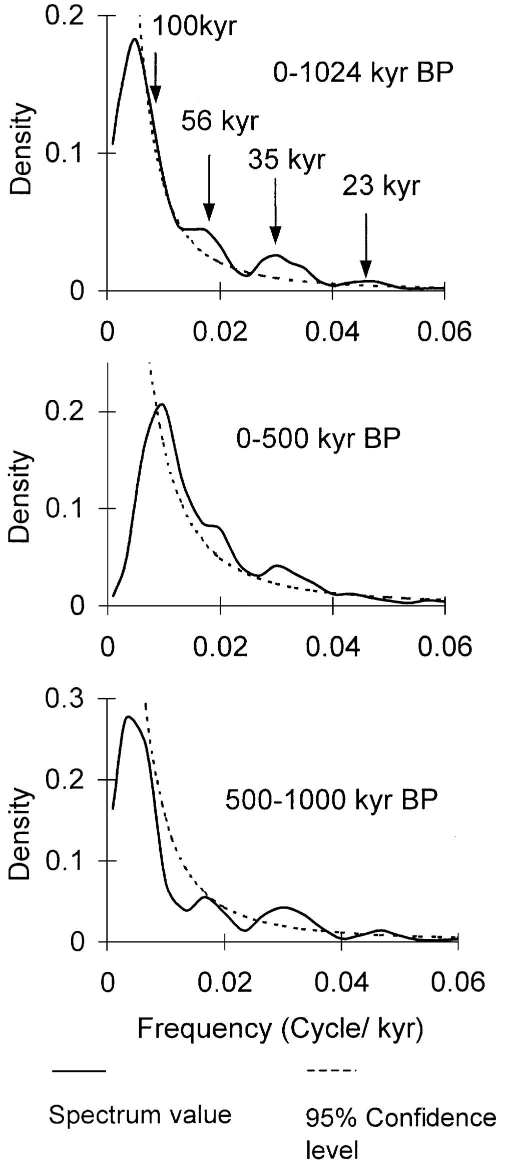

Fig. 3. Blackman–Tukey spectral analysis of the winter monsoon time series of the past million years.

may cause these cycles in the monsoon systems (King, 1996), though this cannot be detected in this study.

4. Discussion

Many investigations using spectral analyses have found the orbital cycles of quasi-100, quasi-55, 41 and 23 ka, as well as orbital or nonorbital ones such as 210 and 35 ka in the Chinese loess record (An et al., 1990; Wang et al., 1990; Kukla et al., 1990; Xu and Liu, 1994; Ding et al., 1994, 1995; Van Huissteden et al., 1997; Lu et al., 1999a). Spurious spectrums may have resulted from unclear time scales and climatic implication of the proxy indicator employed (An et al., 1990; Wang et al., 1990; Kukla et al., 1990; Xu and Liu, 1994). Van Huissteden et al. (1997) have developed an absolute time series which was spectrally analyzed, but the MESA and MTM methods they used cannot detect the time evolution of the cycles, such as the strength of the quasi-100- and quasi-220-ka cycles shift in the time series found in this study. Our wavelet transform results and comparison with the traditional Fourier-based analysis offer a new view of characteristics of the monsoon changes in the past million years. Both methods show common cycles of quasi-100, quasi-55 and 25–18 ka. The quasi-100-, 55- and 23-ka cycles detected by our spectral analyses are consistent with those of Van Huissteden et al. (1997).

There is no predominant 41-ka cycle in our results from both wavelet transform and spectral analysis, although the 41-ka cycle was found in the previous studies (An et al., 1990; Xu and Liu, 1994; Ding et al., 1995; Van Huissteden et al., 1997). The spectral analysis on an orbitally tuned time scale may not offer accurate frequency information of the time series (Ding et al., 1995). Difference in the 41-ka orbital cycle between Van Huissteden's spectral result with our analyses may be due to a twice-longer (2 million) grain-size time series used by them. It is possible that the 41-ka cycle is not strong during the past 1000 ka, but it is dominant over the 1000–2000 ka BP period. The cause of the absence of a 41-ka cycle in the East Asian winter monsoon system during the past million years may be different to the India monsoon system. The India monsoon system is strongly driven by the low-latitude precession variations (Clemens et al., 1991), while the East Asian winter monsoon should be primarily driven by the higher latitude obliquity cycle, and thus the 41-ka cycle is not well preserved. The absence of a 41-ka cycle in the East Asian winter monsoon system may be strongly related to the interaction between the ice volume changes of the northern hemisphere and the moist atmospheric current from oceans at the lower latitude (An et al., 1990; Ding et al., 1995). For example, the East Asian summer monsoon circulation, which brings the moisture from the low-latitude oceans, may modulate the climate change in the Loess Plateau. Thus, the mixture of the several aspects could shade the 41-ka cycle in the record. It is very unlikely that the imperfect time scale has caused the absence of 41-ka cycle because the time series developed in this study is one of the best for the Chinese loess deposit at present. The accurate location of the B/M boundary of Kukla and An (1989) has been recently suspected, though never been confirmed, because of the unclear acquisition magnetism of the loess (Zhu et al., 1998; Zhou and Shackleton, 1999). This may cause spurious frequencies in our study. Although this will not change the cycles of the time series, it can be corrected when the B/M boundary is fixed in the future.

CWT results clearly show that the cycles of the monsoon system shifted at around 500 ka BP. This climatic shift is supported by the geological observation of the Chinese loess deposit (Liu, 1985; Kukla and An, 1989; An et al., 1990; Ding et al., 1994; Vandenberghe et al., 1997; Lu et al., 1999a). The measurement of environment proxy indexes of Chinese loess deposit shows that the past 500 ka is shown in stronger glacial–interglacial changes compared to its previous climatic regime. The strong variation of the monsoon system during 500–0 ka BP may show that the boundary condition of the monsoon system was changed, as compared with the previous condition. The strengthened winter monsoon episodes in Fig. 2 correspond quite well to the highest dust sedimentation rate, such as at the loess deposit period of L9 (9th loess unit). Also, the weakening winter monsoon episodes correlate well with the developed paleosol unit, such as at the paleosol deposit of S5 (5th buried soil) (Fig. 2). The reason of this significant climatic shift around 500 ka BP is not clear. It might be related to the ocean current (which is an important part of the East Asian winter monsoon system) changes and tectonic movement (such as the Tibetan uplift), and/or it could well be the internal variation of the climate system.

5. Conclusions

On the bases of sedimentation rate model and the palaeomagnetic dates, an absolute (not orbitally tuned) grain-size time series of Chinese loess has been obtained. Wavelet analyses on the time series show that the patterns and frequencies of the East Asian winter monsoon climate vary with time during the past million years. There are quasi-200-, 130–110-, 60–50- and 25–18-ka periods/cycles in the winter monsoon changes. A shift of climatic pattern from predominantly quasi-200- to quasi-100-ka cycle at around 500 ka BP is revealed by the wavelet analyses. This climatic shift is also supported by previous studies of the geological records. Traditional spectral analysis on this same time series shows that the East Asian winter monsoon changes mainly at Milankovich cycles, but there are also cycles which may not be explained by orbital forcing. The predominant 41-ka cycle identified by previous investigations is not evident in our time series from both the wavelet and spectral analyses. Our results present new evidence that not only solar radiation, but also other boundary conditions, may have forced the monsoon system changes at the 10^4–10^5 years time scale.

Acknowledgements

The authors are grateful to Dr. Ko Van Huissteden and an anonymous reviewer for their insightful comments which lead to significant improvement of our early manuscript. Thanks also go to Prof. Zhisheng An and Prof. Jef Vandenberghe who arranged the field and laboratory works, to Dr. Ziwang Deng and Dr. Li Li for their helpful suggestions and to Mr. Yanjun Cai for his help in printing Fig. 2. This research is under the auspices of the Chinese Academy of Sciences (KZCX1-10-01 and KZCX2-SW-118), National Key Project for Basic Research (G199804800) and the Dutch Academy of Sciences.

References

An, Z.S., Liu, T.S., Lu, Y.C., Porter, S.C., Kukla, G., Wu, X.H., Hua, Y.M., 1990. The long-term palaeomonsoon variation recorded by the loess–paleosol sequence in central China. Quaternary International 7, 91–95.

An, Z.S., Porter, S.C., Kukla, G., Xiao, J.L., 1991. Late Quaternary dust flow on Chinese Loess Plateau. Catena 18, 125–132.

Blackman, R.B., Tukey, J.W., 1958. The Measurement of Power Spectra, from the Point of View of Communications Engineering. Dover Publications, New York, 190 pp.

Bolton, E.W., Maasch, K.A., Lilly, J.M., 1995. A wavelet analysis of Plio–Pleistocene climate indicators: a new review of periodicity evolution. Geophysics Research Letter 22 (20), 2753–2756.

Cande, S.C., Kent, D.V., 1992. A new geomagnetic polarity time scale for the late Cretaceous and Cenozoic. Journal of Geophysical Research 97 (B10), 13917–13951.

Clemens, S., Prell, W., Murray, D., Shimmield, G., Weedon, G., 1991. Forcing mechanisms of the Indian Ocean monsoon. Nature 353, 720–725.

Ding, Z.L., Yu, Z.W., Rutter, N.W., Liu, T.S., 1994. Towards an orbital time scale for Chinese loess deposit. Quaternary Science Reviews 13, 39–70.

Ding, Z.L., Yu, Z.W., Liu, T.S., 1995. Ice-volume forcing of East Asian winter monsoon variations in the past 800,000 years. Quaternary Research 44, 149–159.

Forman, S.L., 1991. Late Pleistocene chronology of loess deposition near Luochuan, China. Quaternary Research 36, 19–28.

Ghil, M., Allen, R.M., Dettinger, M.D., Ide, K., Kondrashov, Mann, M.E., Robertson, A., Saunders, A., Tian, Y., Varadi, F., Yiou, P., 2002. Advanced spectral methods for climatic time series. Review of Geophysics, submitted for publication.

King, T., 1996. Quantifying non-linearity and geometry in time series of climate. Quaternary Science Reviews 15, 247–266.

Kukla, G., An, Z.S., 1989. Loess stratigraphy in central China. Palaeogeography, Palaeoclimatology, Palaeoecology 72, 203–223.

Kukla, G., An, Z.S., Meliece, L., Gavin, G., Xiao, J.L., 1990. Magnetic susceptibility record of Chinese loess. Transactions of the Royal Society of Edinburgh. Earth Sciences 81, 263–288.

Lau, K.M., Weng, H.Y., 1995. Climate signal detection using wavelet transform: how to make a time series sing. Bulletin of the American Meteorological Society 76 (12), 2391–2402.

Li, J.J., Feng, Z.D., Tang, L.Y., 1988. Late Quaternary monsoon patterns on the Loess Plateau of China. Earth Surface Processes and Landforms 13, 125–135.

Liu, T.S., 1985. Loess and Environment. China Ocean Press, Beijing, pp. 149–157.

Liu, H.S., Chao, B.F., 1998. Wavelet spectral analysis of the earth's orbital variations and paleoclimatic cycles. Journal of the Atmospheric Sciences 55 (2), 227–236.

Liu, T.S., Ding, Z.L., 1998. Chinese loess and the palaeomonsoon. Annual Reviews of Earth and Planetary Sciences 26, 111–145.

Lu, H.Y., An, Z.S., Vandenberghe, J., Nugteren, G., 1997. Evidence for paleoclimatic significance of grain size composite of loess deposit in central Chinese Loess Plateau. In: An, Z.S., Zhou, W.J. (Eds.), Proc. 30th Int'l Geol. Congr., vol. 21. VSP Press, The Netherlands, pp. 5–10.

Lu, H.Y., Liu, X.D., Zhang, F., An, Z.S., Dodson, J., 1999a. Astronomical calibration of loess–paleosol deposits at Luochuan, central Chinese Loess Plateau. Palaeogeography, Palaeoclimatology, Palaeoecology 154, 237–246.

Lu, H.Y., Huissteden, K.V., An, Z.S., Nugteren, G., Vandenberghe, J., 1999b. East Asian winter monsoon changes on millennial time scale before the last glacial–interglacial cycle. Journal of Quaternary Science 14, 101–110.

Lu, H.Y., Huissteden, K.V., Zhou, J., Vandenberghe, J., Liu, X.D., An, Z.S., 2000. Variability of East Asian winter monsoon in Quaternary climatic extremes in North China. Quaternary Research 54, 321–327.

Maher, B.A., Thompson, R., 1992. Palaeoclimatic significance of the magnetic record of the Chinese loess and paleosols. Quaternary Research 37, 155–170.

Morley, J.J., Heusser, L.E., 1997. Role of orbital forcing in east Asian monsoon climates during the last 350 kyr: evidence from terrestrial and marine climate proxies from core RD14-99. Paleoceanography 12, 483–493.

Pisias, N.G., Rea, D.K., 1988. Late Pleistocene palaeoclimatology of the central equatorial Pacific: sea surface response to the southeast trade winds. Paleoceanography 3, 21–37.

Porter, S.C., An, Z.S., 1995. Correlation between climate events in the North Atlantic and China during the last glaciation. Nature 375, 305–308.

Sun, Y.B., Lu, H.Y., An, Z.S., 2000. Grain size distribution of quartz isolated from Chinese loess/paleosol. Chinese Science Bulletin 45, 2296–2298.

Vandenberghe, J., An, Z.S., Nugteren, G., Lu, H.Y., Huissteden, K.V., 1997. New absolute time scale for the Quaternary climate in the Chinese loess region by grain-size analysis. Geology 25, 35–38.

Van Huissteden, J., Nugteren, G., Vandenberghe, J., An, Z.S., 1997. Spectral analysis of a grain size record of the loess deposits in central China. In: Zhang, Z., et al., (Eds.), Proc. 30th Int'l Geol. Congr., vol. 2. VSP, The Netherlands, pp. 313–325.

Wang, Y., Evans, M.E., Rutter, N., Ding, Z., 1990. Magnetic susceptibility of Chinese loess and its bearing on paleoclimate. Geophysical Research Letters 17 (2), 2449–2451.

Weng, H.Y., Lau, K.M., 1994. Wavelets, period doubling, and time-frequency localization with application to organization of convection over the tropical western Pacific. Journal of Atmospheric Sciences 51, 2523–2541.

Xu, T.C., Liu, T.S., 1994. Implication of the magnetic susceptibility curve from the Chinese loess profile at Xifeng. Quaternary Science Reviews 12, 249–254.

Zhang, X.Y., An, Z.S., Chen, T., Zhang, G.Y., Arimotoand, R., Ray, B.J., 1994. Late Quaternary records of the atmospheric input of aeolian dust to the center of the Chinese Loess Plateau. Quaternary Research 41, 35–43.

Zhang, X.Y., Arimoto, R., An, Z.S., 1999. Glacial and interglacial patterns for Asian dust transport. Quaternary Science Reviews 18, 811–819.

Zhou, L.P., Shackleton, N.J., 1999. Misleading positions of geomagnetic reversal boundaries in Eurasian loess and implication for correlation between continental and marine sequences. Earth and Planetary Sciences Letters 168, 117–130.

Zhou, L.P., Oldfield, F., Wintle, A.G., Robinson, S.G., Wang, J.T., 1990. Partly pedogenic origin of magnetic variations in Chinese loess. Nature 346, 737–739.

Zhu, R.X., Pan, Y.X., Guo, B., Liu, Q.S., 1998. A recording phase lag between ocean and continent climate changes: constrained by the Matuyama/Brunhes polarity boundary. Chinese Science Bulletin 43 (19), 1593–1598.